

# Energy Efficiency and Greenhouse Gas Emission Intensity of Petroleum Products at U.S. Refineries

Amgad Elgowainy,<sup>†</sup> Jeongwoo Han,<sup>†</sup> Hao Cai,<sup>†</sup> Michael Wang,<sup>†</sup> Grant S. Forman,<sup>\*,‡</sup> and Vincent B. DiVita<sup>§</sup>

<sup>†</sup>Systems Assessment Group, Energy Systems Division, Argonne National Laboratory, 9700 South Cass Avenue, Argonne, Illinois 60439, United States

<sup>‡</sup>Sasol Synfuels International, 900 Threadneedle, Suite 100, Houston, Texas 77079, United States

<sup>§</sup>Jacobs Consultancy Inc., 5995 Rogerdale Road, Houston, Texas 77072, United States

## S Supporting Information

**ABSTRACT:** This paper describes the development of (1) a formula correlating the variation in overall refinery energy efficiency with crude quality, refinery complexity, and product slate; and (2) a methodology for calculating energy and greenhouse gas (GHG) emission intensities and processing fuel shares of major U.S. refinery products. Overall refinery energy efficiency is the ratio of the energy present in all product streams divided by the energy in all input streams. Using linear programming (LP) modeling of the various refinery processing units, we analyzed 43 refineries that process 70% of total crude input to U.S. refineries and cover the largest four Petroleum Administration for Defense District (PADD) regions (I, II, III, V). Based on the allocation of process energy among products at the process unit level, the weighted-average product-specific energy efficiencies (and ranges) are estimated to be 88.6% (86.2%–91.2%) for gasoline, 90.9% (84.8%–94.5%) for diesel, 95.3% (93.0%–97.5%) for jet fuel, 94.5% (91.6%–96.2%) for residual fuel oil (RFO), and 90.8% (88.0%–94.3%) for liquefied petroleum gas (LPG). The corresponding weighted-average, production GHG emission intensities (and ranges) (in grams of carbon dioxide-equivalent (CO<sub>2e</sub>) per megajoule (MJ)) are estimated to be 7.8 (6.2–9.8) for gasoline, 4.9 (2.7–9.9) for diesel, 2.3 (0.9–4.4) for jet fuel, 3.4 (1.5–6.9) for RFO, and 6.6 (4.3–9.2) for LPG. The findings of this study are key components of the life-cycle assessment of GHG emissions associated with various petroleum fuels; such assessment is the centerpiece of legislation developed and promulgated by government agencies in the United States and abroad to reduce GHG emissions and abate global warming.



## 1. INTRODUCTION

**1.1. U.S. Refineries.** In 2012, U.S. refineries processed an average of 15 million barrels (bbl)/day of crude and 2.5 million bbl/day of natural gas liquids (NGLs) and other liquids and blending components to produce a total of 18.5 million bbl/day of finished products. The average utilization for crude processing was 89% of total U.S. refining capacity.<sup>1</sup> The majority of the refining and blending products are finished motor gasoline (8.9 million bbl/day), distillate fuel oil (4.6 million bbl/day), and jet fuel (1.5 million bbl/day), which comprise 15 million bbl/day of clean products with a gasoline-to-diesel ratio (G/D) of approximately 2:1.<sup>2</sup> The energy consumption of the refinery industry was 3540 trillion British thermal units (Btu) in 2012, and the industry generated 173 million metric tons of carbon-dioxide-equivalent (CO<sub>2e</sub>) emissions.<sup>3,4</sup> Refinery operations are impacted by many factors, including crude prices, sources, and quality; market demand for finished products; fuel prices in world markets; and state and federal regulations.

**1.2. Fuel Sources and Characteristics.** The *Annual Energy Outlook* (AEO), prepared by the Energy Information Administration (EIA), estimates that crude supply to U.S. refineries will decline from 15.0 million bbl/day in 2012 to 14.3 million bbl/day in 2020 and 13.7 million bbl/day in 2030 as a result of reduced gasoline demand.<sup>5</sup> The AEO also predicts that domestic crude production will increase from 6.3 million bbl/day in 2012 to 7.5 million bbl/day in 2020 then decrease back to about 6.3 million bbl/day in 2030. Net crude imports are estimated to decline from 8.5 million bbl/day in 2012 to 6.8 million bbl/day in 2020, then increase to 7.3 million bbl/day by 2030. This increase in domestic crude production in the next decade is attributed to increased production that results from onshore exploration of tight and shale oil formations.<sup>5</sup> Coupled with the projected

Received: February 28, 2014

Revised: May 19, 2014

Accepted: May 28, 2014

Published: May 28, 2014

increase in oil sands imports from Canada, crude imports from other parts of the world are expected to decrease significantly.

Crude produced from shale oil is generally light and sweet (low sulfur content), while bitumen produced from oil sands is heavy and sour (high sulfur content). The bitumen requires further upgrading or dilution, resulting in changes in the quality of the crude that will supply U.S. refineries in different Petroleum Administration for Defense District (PADD) regions. The demand for gasoline blendstock is projected to decrease with the more stringent Corporate Average Fuel Economy (CAFE) standards for light-duty vehicles (54.5 miles per gallon by model year 2025<sup>6</sup>) and the increase in biofuels used in blending.<sup>7</sup> However, the demand for diesel fuel is expected to increase with economic growth.<sup>8</sup> More stringent regulation of emissions from locomotives, marine vessels, and other transportation and stationary applications<sup>9</sup> will increase the demand for ultralow sulfur diesel, which will require more intensive refining operations and/or the use of synthetic fuels such as Fischer–Tropsch (FT) diesel for blending to meet diesel fuel specifications. The variations in American Petroleum Institute (API) gravity and sulfur content (sulfur wt %) of crude oil that will result from the expected change in crude oil sources to U.S. refineries and the decline in G/D ratio will likely change the way refineries plan and optimize their operations. In addition, low natural gas (NG) prices may contribute to future refinery upgrades (e.g., installation of hydrocracking units) to process the increased share of heavier crude and meet the required hydrogen/carbon ratio for desired products while achieving fuel specification standards.<sup>10</sup>

**1.3. Fuel Regulations and Standards.** The California Low-Carbon Fuel Standard (LCFS) requires fuel producers and importers who supply or sell motor gasoline or diesel fuel in California to reduce, by 2020, the carbon intensity of transportation fuels (measured in grams of CO<sub>2e</sub> emissions per megajoule (MJ) of produced fuel on a life-cycle basis) by an average of 10% from 2010 levels.<sup>11</sup> Carbon intensity is the measure of greenhouse gas (GHG) emissions associated with producing, transporting, and consuming a unit of fuel energy (e.g., grams of CO<sub>2e</sub>/MJ) on a life-cycle basis. The Energy Independence and Security Act of 2007 established a Renewable Fuel Standard (RFS) with volume requirements for several categories of renewable transportation fuels. The RFS program requires the production of 36 billion gallons of renewable fuels for use and blending into transportation fuels by 2022. Each renewable fuel type in the RFS program must achieve minimum life-cycle GHG emission reductions relative to the petroleum fuel it replaces.<sup>7</sup> Both the California LCFS and the EPA RFS assess alternative fuels against carbon intensities of petroleum-derived gasoline and diesel for policy implementation. The Renewable Energy Directive promulgated by the European Union requires a minimum threshold on emissions savings from biofuels compared with fossil fuels based on a life-cycle analysis. The current GHG emissions savings from the use of biofuels must be at least 35% compared with petroleum fuels; this requirement increases to 60% in 2018.<sup>12</sup> Estimating the relative GHG emissions reductions associated with alternative fuels requires reliable estimates of the GHG emissions generated by production of the petroleum fuels that will be displaced.

## 2. PREVIOUS STUDIES

The major stages in the life cycle of a petroleum fuel include crude recovery, refining, and fuel combustion. GHG emissions from fuel combustion (the largest emission source) can be

accurately estimated by balancing the carbon in the fuel and the products. The second-largest GHG emission source in the petroleum fuels pathways is the petroleum refining process. Overall refinery efficiency is the ratio of the energy present in all product streams divided by the energy in all input streams. Although overall energy efficiency at the refinery level can be accurately estimated, a method is required to allocate the refinery's total energy use and emissions among the various refined fuel products. Evaluating the energy and emissions burden of individual refinery products, especially fuel products, is necessary to satisfy regulations such as the California LCFS and allow life-cycle comparisons of petroleum fuels and new alternative fuels.

Furuholt (1995) applied an allocation method based on eight general refining processes in Norwegian refineries.<sup>13</sup> Furuholt demonstrated that energy use and emissions calculated for individual refinery products based on process unit-level allocations are significantly different from those obtained from aggregate refinery-level-based allocation. Wang et al. (2004) presented a petroleum refinery process-based approach to allocating energy use in a refinery to individual products based on mass, energy content, and market value share of final and intermediate petroleum products as they flow through refining process units.<sup>14</sup> They used results from a notional refinery to estimate process-level operations and energy burdens. Skone and Gerdes (2009) attempted to allocate refineries' energy use and emissions to gasoline, diesel, and jet fuels using (1) aggregate data from EIA on process unit throughput and (2) 1996 data from an API/National Petroleum Refiners Association survey on aggregate inputs to the vacuum distillation, hydrotreating, catalytic reforming, alkylation, and isomerization units.<sup>15</sup>

Bredeson et al. (2010) examined the factors driving refinery CO<sub>2</sub> emission intensity and allocated these emissions to individual products.<sup>16</sup> They described a detailed model of a refinery in which individual process unit throughputs could vary without constraints to determine CO<sub>2</sub> emissions as a function of key operational parameters. Bredeson et al. revealed that the most important factor driving a refinery's energy requirement is the hydrogen (H<sub>2</sub>) content of the products in relation to the H<sub>2</sub> content of the crude. They found that the total refinery emissions did not change as the refinery shifted from gasoline to diesel production and concluded that the reformer is an energy/CO<sub>2</sub>-equalizing device, shifting energy/CO<sub>2</sub> from gasoline into distillates. Bredeson et al. proposed a modified allocation method that includes an H<sub>2</sub> transfer term to provide energy and emissions results consistent with the refinery behavior. Keesom et al. (2009) used a first-principles engineering approach in investigating the differences in emissions of various crudes from production through the refinery process.<sup>17</sup> Abella and Bergerson (2012) developed a petroleum refinery model to quantify energy use and GHG emissions for a range of crude oil properties, with a focus on oil sands products, for different refinery configurations.<sup>18</sup> Hirshfeld and Kolb (2012) used linear programming modeling of the U.S. refining sector to estimate total annual energy consumption and CO<sub>2</sub> emissions in 2025 for four projected U.S. crude oil slates. They projected the U.S. refinery energy use to increase by 3.7%–6.3% and refinery CO<sub>2</sub> emissions to increase by 5.4%–9.3% compared to the baseline.<sup>19</sup>

Although previous studies provided valuable input to the understanding of the variation in product-specific energy and GHG emission intensities for a given refinery model, they were based on models of notional refineries, and thus may not have captured the variations within the U.S. refining industry. Further,



direct processing energy use at U.S. refineries was refinery fuel gas (FG), 25% NG, 13% captive (i.e., produced internally) and merchant (i.e., purchased) hydrogen, 14% refinery catalytic coke, 6% purchased steam, 4% purchased electricity, and 1% other fuels.<sup>3</sup> Virtually all purchased hydrogen is produced via steam methane reforming (SMR) of natural gas, making NG the largest contributor to total energy use in U.S. refineries. The objective of an oil refinery is to distill the supplied crude into fractions and chemically transform the fractions into products that meet product specifications. To achieve that objective, a petroleum refinery utilizes a set of process units that convert relatively low-value liquid hydrocarbons (e.g., crude oil, vacuum gas oil, and natural gasoline) into more valuable “clean” products such as gasoline, diesel, and jet fuel by modifying the hydrogen-to-carbon ratio of the various feeds in process units. Figure 1 is a schematic of a refinery showing major process units and their inputs and outputs. In a refinery, a distillation process separates the crude into groups of molecules with a particular boiling temperature range. Each group is sent to different process units, where catalytic and thermal processes modify the carbon/hydrogen bonds and ratios of hydrocarbons while eliminating undesired components such as sulfur and nitrogen. Blending components such as ethanol, reformates, and alkylates, etc., are often added to satisfy the volume and quality requirements of each end product. Each refining unit has a different energy requirement depending on feedstock and end-product requirements and specifications. Part of the energy demand is met by combustion of intermediate refining products (e.g., FG and catalytic coke), while the remaining energy requirement is

satisfied with purchased electricity, steam, and NG. Refineries also consume large quantities of hydrogen that is produced on-site via SMR of NG and/or through purchased (merchant) hydrogen.

**3.1.1. Overall Refinery-Level Energy Efficiency.** In the current study, we developed LP data on the material and energy inputs and outputs of 43 U.S. refineries representing 70% of total U.S. refined crude in 2012 (Table 1). Refinery LP modeling is a process-oriented representation of refinery operations, the material flows between refining processes, the prices of inputs and outputs, and refineries’ technical and economic responses to changes in requirements dictated by petroleum product specifications, such as the vapor pressure and octane rating of gasoline.<sup>19</sup> The LP model maximizes refinery profit by determining the optimal volumetric throughput and utility balance (i.e., product slate, fuel gas, electricity, steam, and water, etc.) among various process units in a refinery under given market and technical conditions (e.g., the prices of inputs and outputs, refinery configurations, fuel specifications and regulations). The volumetric and mass input and output results from LP modeling can be converted into energy balance results with product heating values. The input and output data from the LP model for each modeled refinery are those listed in eq 1 below. The LP model results are validated against propriety data from the refining industry and refinery statistical data provided by EIA.

Using eq 1, we estimated the overall energy efficiency of individual refineries based on the total energy input and output on a lower heating value (LHV) basis.

$$\eta_{\text{LHV}} = \frac{\sum_n (P_n \times \text{LHV}_n)}{\sum_m (C_m \times \text{LHV}_m) + \sum_o (\text{OI}_o \times \text{LHV}_o) + \text{NG}_{\text{purchased, LHV}} + \text{H}_{2, \text{purchased, LHV}} + \text{Electricity}_{\text{purchased}}} \quad (1)$$

where  $\eta_{\text{LHV}}$  is the LHV-based overall efficiency of a refinery;  $P_n$  is the amount of refining product  $n$  (e.g., gasoline, jet fuel, diesel,

**Table 1. Coverage of Crude Input to Refineries by LP Modeling for Each PADD Region**

PADD region	crude input to refineries evaluated with LP modeling (1000 bbl/day)	crude input to refineries (1000 bbl/day) <sup>a</sup>	coverage of LP modeling (%)
I	404	921	44
II	2150	3451	62
III	5983	7755	77
IV	-	574	0
V	1956	2337	84
total	10,493	15,038	70

<sup>a</sup>From EIA (2013) for 2012.<sup>1</sup>

liquefied petroleum gas (LPG), and residual fuel oil (RFO)), in bbl;  $C_m$  is the amount of crude input  $m$ , in bbl;  $\text{OI}_o$  is the amount of other input material  $o$  (e.g., normal butane, iso-butane, reformate, alkylate, and natural gasoline), in bbl;  $\text{NG}_{\text{purchased, LHV}}$  is the LHV-based energy of purchased NG (in the case of purchased steam, it is combined with NG, and a boiler efficiency of 80% is assumed);  $\text{H}_{2, \text{purchased, LHV}}$  is the LHV-based energy of purchased hydrogen;  $\text{Electricity}_{\text{purchased}}$  is the energy in purchased electricity; and  $\text{LHV}_m$ ,  $\text{LHV}_n$ , and  $\text{LHV}_o$  are the LHVs of crude input  $m$ , refining product  $n$ , and other input material  $o$ , respectively, in million Btu per barrel.

For comparison, we generated refinery efficiencies using aggregate EIA refinery data at the PADD level. EIA publishes annual statistics on volumetric crude oil and blending stock inputs, use of combined captive and merchant hydrogen, consumption of FG and other process fuels (e.g., catalytic coke and NG), use of purchased electricity and steam, and refining product outputs of refineries in various PADD regions. Equation 1 was applied to estimate refining efficiencies using EIA and LP modeling data for the year 2010.

**3.1.2. Refinery Characterization.** As shown in Table 2, the 43 modeled refineries differed in terms of their sources and properties of crude oil, their configuration complexity, and their finished product slate. Crude quality affects the type and intensity of processes needed to transform the crude into final products. The refinery configuration reflects the required processing technologies for the desired slate of final products. Crude API gravity is a measure of the density of crude oil. Compared with low-API crude, high-API crude is less dense (i.e., lighter) and contains higher proportions of small molecules, which can be more readily processed into gasoline, jet fuel, and diesel. Heavier crudes generally require more energy to be processed into final products compared with lighter crudes because of their low hydrogen content and the need for additional conversion processes.

Most of the sulfur in crude oil must be removed in the refining process, primarily through hydrotreatment (see Figure 1) to meet each product’s sulfur specifications and comply with environmental regulations. Therefore, API gravity and sulfur



**Table 2. Operational Characteristics of the 43 Modeled Refineries, by Region**

	API gravity	sulfur (wt %)	G/D ratio <sup>b</sup>	HP yield (%) <sup>c</sup>	complexity index
PADD I					
weighted average <sup>a</sup>	34.7	1.2	2.2	7	9.4
minimum	32.9	0.5	1.7	6	9.1
maximum	35.9	2.1	2.5	9	9.9
PADD II					
weighted average <sup>a</sup>	28.6	2.0	2.1	14	10.1
minimum	21.5	0.5	1.6	5	8.8
maximum	39.1	3.0	2.7	19	12.6
PADD III					
weighted average <sup>a</sup>	28.1	2.1	1.8	8	10.8
minimum	20.3	0.5	1.1	4	7.8
maximum	36.4	3.5	2.7	12	13.4
PADD V					
weighted average <sup>a</sup>	24.9	1.3	2.7	17	11.9
minimum	16.2	0.9	1.5	7	7.0
maximum	33.1	1.7	5.4	25	15.4
43 Refineries					
average	27.9	1.9	2.0	11	10.8
minimum	16.2	0.5	1.1	4	7.0
maximum	39.1	3.5	5.4	25	15.4

<sup>a</sup>Volume of crude oil (inputs basis). <sup>b</sup>The volumetric ratio of gasoline yield to diesel yield (G/D). <sup>c</sup>The yield of heavy products (HP) (i.e., residual fuel oil, pet coke, asphalt, slurry oil and reduced crude) as a share of all energy products (by energy value).

content have significant impacts on a refinery's energy use and its overall efficiency. Every individual refinery has a unique configuration and mode of operation. The physical configuration of a refinery can be expressed by a Complexity Index, which is a numerical score that represents the extent, capability, and capital intensity of a given refinery's process units.<sup>19</sup> In general, the higher a refinery's Complexity Index, the greater the refinery's ability to convert more of the heavy fractions of crude into lighter, high-value products, and to produce light products that meet more stringent quality specifications (e.g., ultralow sulfur fuels).<sup>19</sup>

Refining product yields and the product slate have a direct impact on the overall refining efficiency. Higher yields of heavy products with higher energy content result in higher refining efficiency. The aggregate efficiency calculated from LP modeling data of the 43 refineries is 90.6%, which is identical to the calculated efficiency for the entire U.S. refining sector based on EIA annual survey data. Comparison (by PADD region) of the refining efficiencies derived from LP modeling with those based on EIA data is provided in the Supporting Information (SI).

To explore the key parameters that impact a refinery's overall energy efficiency, we conducted linear multivariate regression analysis. The crude oil API and sulfur content are used to characterize crude quality because (1) crude API is known to correlate with various product yields and (2) sulfur content is associated with increased energy consumption in refineries (mainly because of hydrogen consumption in the hydrotreating processes). A certain combination of refinery products (e.g., gasoline, diesel, jet fuel, RFO, asphalt, and coke) can represent the refining product slate for a given refinery. The Complexity Index was used to reflect the refinery complexity.<sup>21</sup> Note that the Complexity Index in this study reflects the throughput of the utilized process units in the modeled refineries.

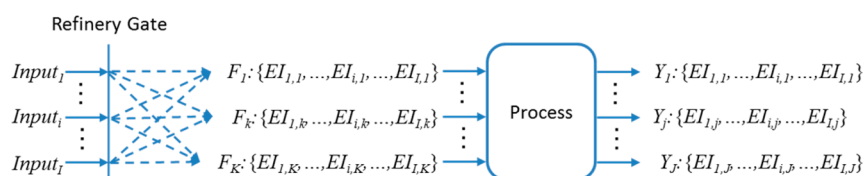
The LHV-based overall efficiencies of the 43 refineries served as data points for the dependent variable, and the influencing factors described above were tested as independent predictors of the linear regression model. A regression model that is statistically acceptable must have statistically significant *P* values (i.e.,  $\leq 0.05$ ) for each individual predictor. Whereas the potential for multicollinearity exists among crude quality, complexity, and finished products, the actual measured degree of multicollinearity in the data set was tested and deemed acceptable. We employed the STATATM statistical tool package<sup>22</sup> to perform the ordinary, least-squares regression with trials comprising various combinations of the potential predictors of overall refining efficiency. The regression with the highest Pearson coefficient (*R*-square) that met the acceptance criteria was constructed as a statistically robust prediction model.

**3.1.3. Regression Formula to Predict Overall Refinery Efficiency.** We constructed a statistically acceptable linear regression model (eq 2) that employed the crude API gravity and the sulfur content, the yield of heavy products (consisting of residual fuel oil, coke and asphalt), and the Complexity Index as predictors.

$$\eta_{\text{LHV}} = 87.59 + 0.2008 \times \text{API} - 0.7628 \times S + 0.07874 \times \text{HP} - 0.1847 \times \text{CI} \quad (2)$$

where  $\eta_{\text{LHV}}$  is the refinery's overall efficiency (on an LHV basis) in %; API is the API gravity of crude oil; *S* is the sulfur content of crude oil in % by weight (e.g., for sulfur content of 6%, *S* = 6); HP is the heavy products yield in % by energy; (e.g., for heavy products yield of 5%, HP = 5); and CI is the actual utilized Complexity Index of the refinery.

The predictors in the regression formula were all statistically significant, at a significance level of 1% ( $p < 0.01$ ). The regression model with the heavy products (HP) yield as a predictor provides a better fit compared with the clean products yield when used as an alternative predictor. The regression formula shows that overall refining efficiency increases with higher crude API, lower crude sulfur content, higher heavy products yield, and a lower refinery Complexity Index. The formula agrees well with the expected cause–effect relationships between a refinery's energy efficiency and the predicting parameters. Lighter crudes

**Figure 2.** Schematic flow of a generic refinery process unit.

processed at less complex refineries require less energy and thus tend to have higher efficiencies, but they also make fewer clean products and more heavy products.

**3.2. Process-Unit-Level Analysis (Process-Level Allocation).** Figure 2 shows a schematic of a generic refinery process unit with various feeds or energy inputs ( $F_1$  through  $F_k$ ) and various yield streams or energy outputs ( $Y_1$  through  $Y_j$ ). Refinery energy inputs (e.g., crude, NG, hydrogen, electricity, and other hydrocarbons (HC)) are denoted by  $Input_i$  in Figure 2. Refinery energy inputs and their derivatives propagate through successive process units (see Figure 1) to produce intermediate products and, eventually, final products. Thus, each stream's energy (feed  $F_k$  or yield  $Y_j$ ) through a process unit carries certain energy burdens associated with the refinery inputs ( $Input_1$  through  $Input_l$ ). For example,  $EI_{ij}$  in Figure 2 denotes the energy burden of a specific refinery input  $i$  that contributes to the production of the unit energy of yield stream  $j$ . The sum of all energy burdens for a particular yield stream  $j$  is defined as the total energy intensity of that stream  $\sum EI_{ij}$  (i.e., the share of the total amount of refinery input energies required to produce the unit energy of that stream). Note that the inverse of energy intensity represents the energy efficiency. By estimating the production energy intensity of all streams and aggregating them for the products that make various final product pools (e.g., gasoline pool, distillate pool), we can obtain final product-specific efficiencies.

For a given process, the energy burden ( $EI_{ij}$  in Btu/Btu) of a refinery input  $i$  to produce the unit energy of a given product yield (stream)  $j$  can be expressed using eq 3:

$$EI_{ij} = \left( \sum_k F_k \times EI_{i,k} \right) \times S_j \div Y_j \quad (3)$$

where  $F_k$  and  $Y_j$  are the energy in feed  $k$  and yield stream  $j$  to and from the process unit (in Btu/day), respectively, while  $S_j$  is the percentage contribution of yield  $j$  in all yield streams ( $Y_1$  through  $Y_j$ ) from a given process unit. The energy and emissions burdens that are allocated to a yield stream  $j$  are defined by  $S_j$ . Note that waste streams such as sulfur are neglected (see SI for a discussion of the sulfur and ethanol adjustment), and thus do not receive any energy or emissions burdens from the process unit.

Common metrics for allocating the energy burdens to a yield stream by its share ( $S_j$ ) in the total yield streams are energy, market value, and mass allocations.<sup>14</sup> In an energy-based allocation, the energy content of each stream is used to calculate its share ( $S_j^E$ ). This is the most commonly used allocation metric in the life cycle of energy products because the significance of energy products is in their energy value. Because market values differ per unit of energy of various fuels, a market-value-based allocation ( $S_j^M$ ) would result in different shares from those calculated on the basis of energy allocation. Some analysts prefer a market value allocation because refinery operation is typically optimized for maximum profit rather than maximum energy efficiency. The market value allocation is impacted by the relative change in market values among various products due to varying market conditions. In Figure S2 of the SI, we show that product-specific efficiencies with energy value and market value allocations are statistically indistinguishable for most refined products. The market values of inputs and outputs of various refinery process units are provided in SI Table S2. In this analysis, mass-based allocation is not applicable because electricity generated from a general utility process cannot be characterized by mass. The energy- and market-value-based shares of a yield stream  $j$  ( $S_j^E$  and  $S_j^M$ , respectively) can be expressed by eq 4:

$$S_j^E = Y_j \div \sum_j Y_j$$

$$S_j^M = Y_j \times \$_j \div \sum_j (Y_j \times \$_j) \quad (4)$$

where  $\$_j$  is the market value of stream  $j$  in \$/Btu. In energy-based allocation,  $EI_{ij}$  can be simplified further, as shown in eq 5:

$$\begin{aligned} EI_{ij} &= \left( \sum_k F_k \times EI_{i,k} \right) \times (Y_j \div \sum_j Y_j) \div Y_j \\ &= \left( \sum_k F_k \times EI_{i,k} \right) \div \sum_j Y_j \end{aligned} \quad (5)$$

Once the process-level allocation is applied to each of the process units in a refinery, the various process units are connected through their input/output relationships. Often, more than two yield streams are pooled into one stream (e.g., FG or hydrogen) and used as feeds to subsequent processes. Even in cases in which the same material is pooled together, their upstream energy burdens are separately tracked because their production pathways are different. After all processes are connected, the energy burdens of all streams in a refinery, including those for the final products, can be obtained. This procedure requires an iterative process because many feedbacks have to converge to develop a stable value.

## 4. RESULTS

**4.1. Overall Refinery-Level Efficiency.** Figure 3 shows that the LHV-based overall efficiencies predicted by the regression

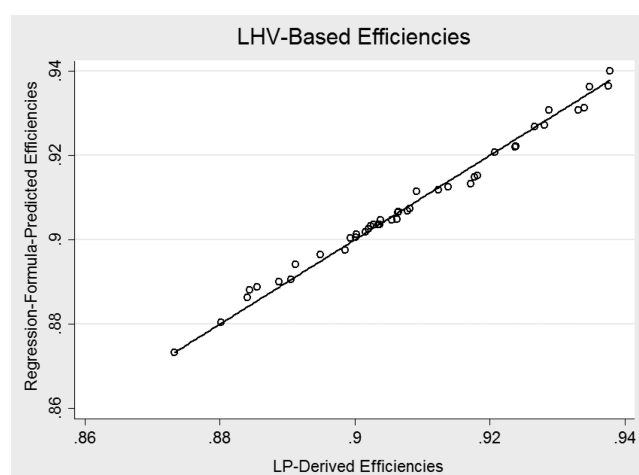


**Figure 3.** Comparison of the LHV-based overall efficiencies predicted by the regression model with those based on LP simulations.

formula agree well with those calculated using eq 2 and LP simulation data. The  $R$ -square value (0.92) of the regression formula implies a high correlation power. When a regression-predicted efficiency ( $X$ ) equals the corresponding LP-derived efficiency ( $Y$ ), the combined pair ( $X,Y$ ) falls on the ( $X=Y$ ) line in Figure 3, implying a perfect prediction. For a given crude quality, a higher refinery Complexity Index (e.g., with coker and/or hydrocracker units) yields smaller amount of heavy products (note their opposite sign in the regression formula (eq 2)). The clean products yield is implied by both the heavy products yield and the Complexity Index in the regression formula (i.e., small amount of heavy products implies greater amount of clean

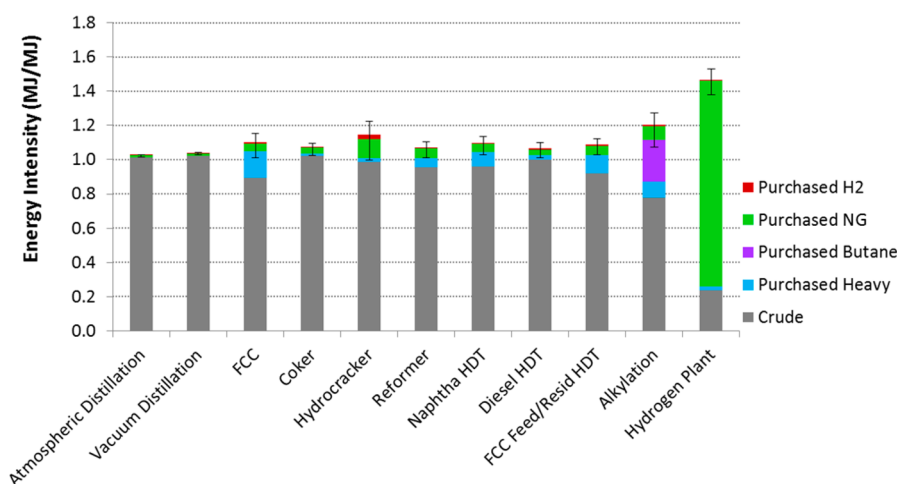


**Figure 4.** Energy intensity of major process units in 43 refineries.

products and vice versa). The gasoline-to-distillate ratio did not deliver an efficiency predictor with statistical significance. This is consistent with the finding of Bredeson et al.<sup>16</sup> that  $G/D$  ratio does not impact the carbon intensity of a refinery within its natural operational constraints.

Note that the regression (correlation) formula (eq 2) should not be used to predict the separate impacts of each parameter on a refinery's overall efficiency because, in practice, these parameters are interdependent and not likely to change independently. Furthermore, note that the correlation formula applies to individual U.S. refineries and only within their natural range of operations (e.g., range of crude and products slates, summer vs. winter operation). Throughout the refining industry, some refiners are more efficient than others because of their design and operation. Two identical refineries with identical crude, complexity, and product slate can have different efficiencies. For example, one refinery might have more sophisticated heat integration or better insulation, thus improving its energy efficiency. Finally, note that the LP data set is representative of the U.S. refining industry, which is the most complex in the world; the applicability of these results to other refining centers around the world requires further investigation.

**4.2. Refinery Process Unit-Level Analysis.** The overall energy efficiency of the entire refinery as a single system provides useful information about the total processing energy use per unit energy in all refinery products. However, this information does not distinguish between the energy intensities of the various refining units that produce the streams that make up the different product pools. Thus, the overall energy efficiency needs to be adjusted by using an energy consumption ratio for each product based on the energy intensity of the process units and their contribution to the various product pools. The following sections address, in detail, the energy intensities of the various processing units and the energy efficiencies and carbon intensities of various refinery products.

**4.2.1. Energy Analysis of Major Processing Units.** We conducted a unit-level analysis based on the LP model's input and output data for each process unit in the 43 refineries. For each of the 43 refineries, the LP model provided volume and mass flow rates (in bbl/day and lb/day, respectively) for all inputs (feeds) and outputs (yields) to and from each process unit, as well as utility consumption. The utility consumption included electricity, steam, and FG. The composition, heating

value, and carbon intensity of refinery FG used in this study are provided in SI Table S3. The electricity consumption value included direct electricity (internally generated from FG) and purchased electricity. Section 3.2 describes the methodology for distributing the overall refinery energy use and emissions among various refinery products to calculate product-specific energy and carbon emissions intensities.

The results from energy- and market-value-based allocations are statistically indistinguishable for all refined products, except for coke (see SI Figure S2). This result is expected because the market values of all major (clean) products (i.e., gasoline, diesel, jet fuel) per unit of their energies are consistent (see SI Table S2). In market value allocation, low-value products such as LPG, RFO, and coke carry smaller energy and emissions burdens compared with the more valuable clean products. However, because of the small shares of these low-value products in the total refinery product pool, the impact of the allocation method on the energy intensity of more-valued fuel products is small (see SI Figure S2). Because the energy contents in the streams represent their main function, the energy allocation method was adopted in this study.

Figure 4 shows the average (and range) of energy intensities for the major processing units in a refinery. The energy intensity of a process unit is defined as the total purchased energy (crude,  $H_2$ , NG, butane, and heavy unfinished oils) that contributed to a unit of energy output from that process. It is calculated by adding the total energy input into a process unit with its upstream burden (up to the refinery gate) and then dividing by the total energy output of that process unit. For example, the hydrogen plant reforms NG to produce hydrogen but requires energy to produce steam for the reforming process. This steam is generated from FG combustion. But FG is not a purchased fuel, and thus must be tracked to one or more of the purchased feeds (i.e., refinery inputs). Figure 4 shows that the origin of most FG used in the hydrogen plant is tracked to crude (e.g., FG from the crude distillation tower or from hydrotreatment of naphtha, which is also produced from crude in the distillation tower; see various pathways that contribute to FG production in Figure 1). Also as shown in Figure 4, a small fraction of the FG for the hydrogen plant originates from the processing of purchased heavy oil (e.g., in the fluid catalytic cracking (FCC) unit). A similar tracking approach calculates the contribution of each purchased input to the production of outputs from each process unit. When hydrogen is used in processing units such as hydrocrackers and

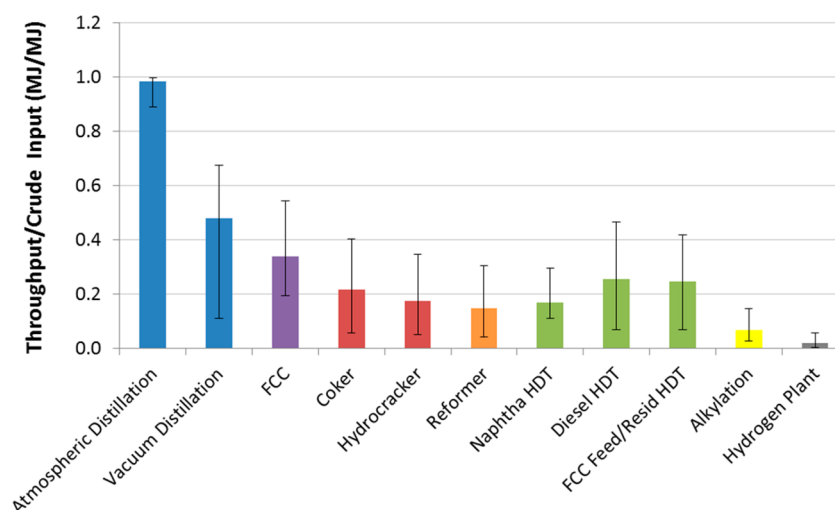


**Figure 5.** Energy throughput from major processing units per unit energy in crude input to 43 refineries.

hydrotreaters (HDTs) (see Figure 1), we account for the different upstream burdens associated with hydrogen production from different sources (e.g., reformer versus SMR plant). The upstream burden of the hydrogen pool is the production-weighted average of the upstream burden associated with each hydrogen production source.

Finally, Figure 4 shows that the hydrogen plant is the most energy-intensive unit in a refinery, followed by alkylation, hydrocracking, gasoline/FCC feed hydrotreaters, and FCC units, respectively. The relative energy intensity of the various process units may appear counterintuitive. For example, the alkylation unit has higher energy intensity compared with the reformer although alkylation occurs near ambient temperature, while high temperatures are required for the reformer. According to the earlier definition of energy intensity, the alkylation unit not only carries its burden of process fuel, but it also carries the upstream burden of its feed sources (up to the refinery gate)—which include the hydrocracker energy allocated to butane and the FCC energy allocated to butane—in addition to the upstream burden of the vacuum and atmospheric towers that feed the hydrocracker and FCC units (see Figure 1). Similarly, the naphtha hydrotreater has higher energy intensity compared with the reformer because of the upstream burden of the naphtha stream from the FCC unit (see Figure 1). Note that a product has a much higher energy intensity when produced at a late refining stage (e.g., naphtha from the FCC unit) compared with production at an early refining stage (e.g., naphtha from the atmospheric distillation tower). The range of energy intensities in Figure 4 for each process unit reflects either the properties of the specific processed input (e.g., the sulfur content in the hydrotreater feed or the API of the hydrocracker feed) or the technology employed for processing (e.g., various technologies of alkylation units).

Figure 5 shows the average throughput from the major refinery units (per unit crude input to the refinery). By combining the throughput ratio with the energy intensity of each unit (Figure 4), we can evaluate the impact of each unit on the overall refinery efficiency. Although the hydrogen plant is the most energy-intensive unit, its yield is small enough to mitigate its impact on overall refinery efficiency. Note that the share of purchased NG for hydrogen production in the 43 modeled refineries is only 15%, with the balance of NG used as a process fuel. Figure 6 shows that 35% of total refining hydrogen demand for the 43

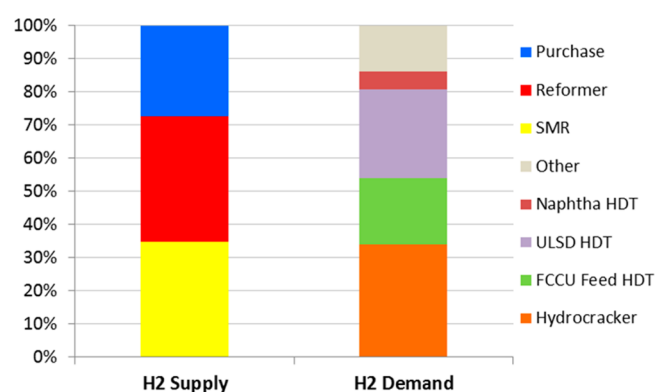


**Figure 6.** Hydrogen supply and demand for major processing units in 43 refineries.

modeled refineries is satisfied by the SMR plant, while 38% is satisfied from the catalytic reformer, and 27% is purchased. The major consumers of hydrogen in a refinery are the hydrocracker and various hydrotreaters.

Whereas the throughput from some processing units contributes directly to the final product pools (e.g., catalytic reformer) (see Figure 1), others contribute only to intermediate products (e.g., hydrogen from the SMR plant). The wide range of throughputs per unit crude input from some processing units reflects the wide variation in refinery configurations, the quality of purchased crude and other inputs, and the slate of finished products across the 43 modeled refineries.

Figure 7 shows the shares of various products from major units in a refinery. As mentioned above, the products could be intermediate (i.e., used as process fuels or require further processing) or final (contributing to various product pools). The yield shares in Figure 7 are separated into five groups:

- Gas, representing C0–C4 molecules (e.g., hydrogen, LPG, and FG);
- Light, representing naphtha and gasoline;
- Middle, representing jet fuel and diesel;
- Heavy, representing heavy and residual oils, coke, and asphalt; and
- Other, such as hydrogen sulfides from hydrotreating units.

Figure 7 shows that almost half of the energy in the crude input is processed in the atmospheric distillation tower into light and



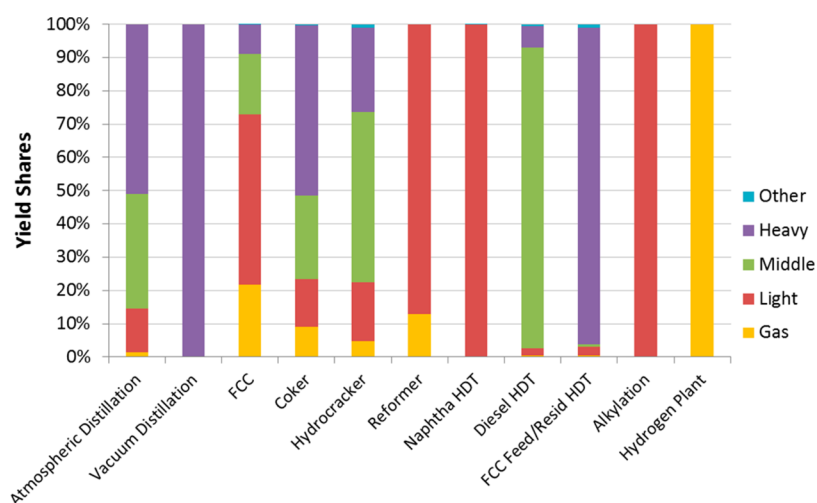


Figure 7. Average product shares (by energy) from major processing units in 43 refineries.

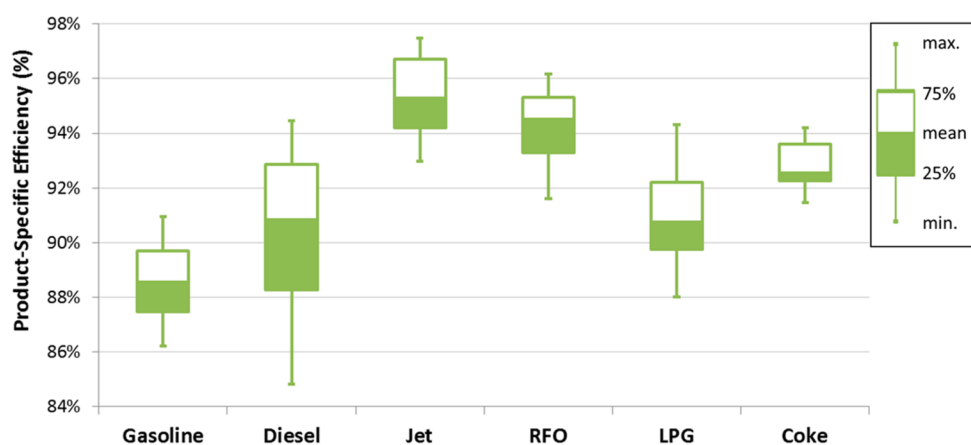


Figure 8. Product-specific efficiency for 43 refineries.

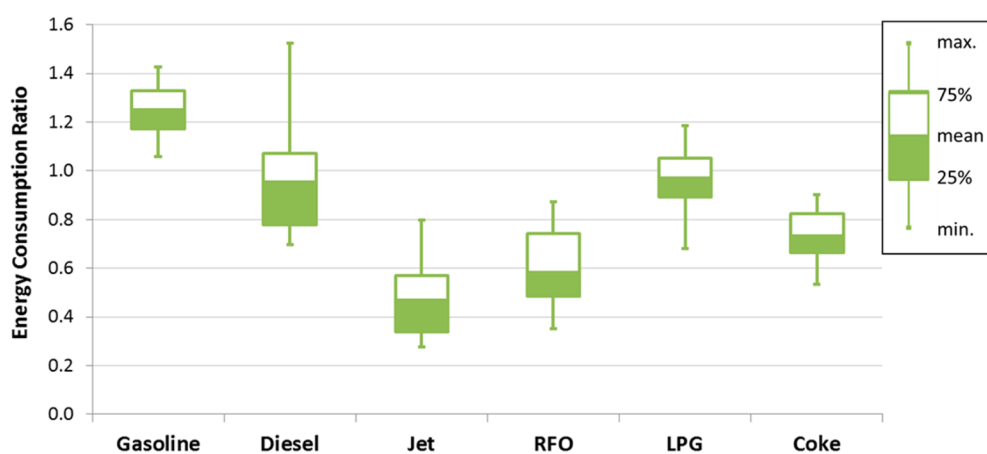


Figure 9. Product-specific energy consumption ratio for 43 refineries.

middle (clean) products, which are further processed in hydrotreaters/reformers before reaching the final product pools. The remaining clean products are produced in the FCC, coker, hydrocracker, and alkylation units, which are more energy-intensive compared with the atmospheric distillation tower (see Figure 4). When combining the product slate from each unit in Figure 7 with the corresponding throughput in Figure 5 for the same units, it becomes clear that most of the diesel (middle) is

produced in the atmospheric distillation tower, hydrocracker, and coker, while most of the gasoline and LPG (light) is produced in the atmospheric distillation tower, FCC, reformer, and alkylation units. Although alkylation, hydrocracking, FCC, and all hydrotreating units are more energy-intensive than other processing units (see Figure 4), they produce higher yield shares of the desired clean products (light and middle) compared with other units (see Figure 7).

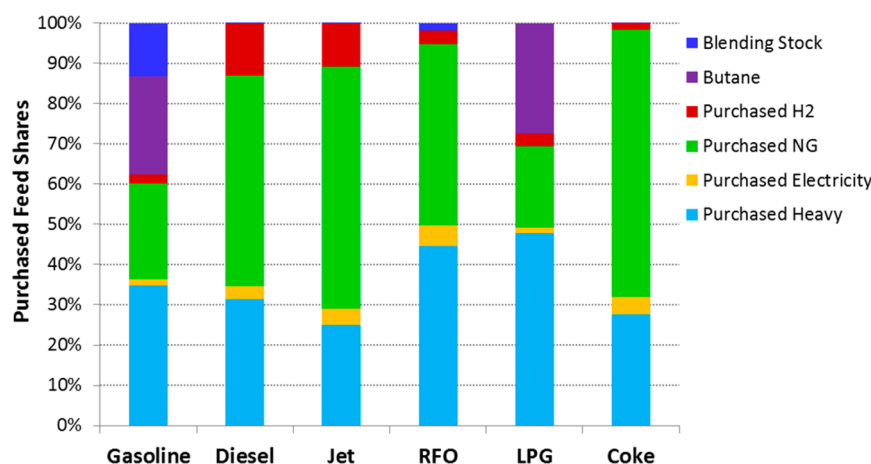


Figure 10. Contribution of purchased feed shares to major refinery products of 43 refineries.

**4.2.2. Analysis of Product-Specific Efficiency and Carbon Intensity.** **4.2.2.1. Product-Specific Efficiency.** Figure 8 shows the calculated average (and distribution) of product-specific efficiencies from the 43 modeled refineries using the energy allocation method. The figure shows a production-weighted average efficiency of 88.6% for gasoline, 90.9% for diesel, 95.3% for jet fuel, 94.5% for RFO, 90.8% for LPG, and 92.6% for coke. The low efficiency of gasoline reflects the high energy intensity of the process units that produce the various streams of the gasoline product pool (e.g., FCC, catalytic reformer, hydrocracker, and alkylation units) (see Figure 4). The vast majority of jet fuel is a straight run from the distillation tower, requiring only hydro-treatment to meet sulfur standards, thus resulting in the highest energy efficiency among all refinery products. Diesel and LPG average efficiencies are similar, but the spread of diesel efficiency is much wider. The wide range of diesel efficiencies is attributable to the various pathways for diesel production in refineries. When less diesel yield is desired, the production pathway becomes more efficient because a larger share of the diesel product is produced directly from the distillation tower. However, when more diesel production is desired, a larger share of the diesel product comes from the hydrocracker (with extensive hydrogen use), the coker, and the FCC units. Furthermore, the more stringent diesel specifications in California require further processing and hydrogen use, thus contributing to the lower end of the diesel efficiency range shown in Figure 8. The wide range in diesel efficiency is discussed in detail in the second paper of this series. LPG efficiency is impacted by the upstream burden of the FCC unit, which produces significant amount of C3 components for LPG production.

Figure 9 shows the calculated energy consumption ratio for individual refinery fuels using LP data for the 43 modeled refineries. The energy consumption ratio for a given product is defined as the product-specific energy intensity relative to the energy intensity for the production of all petroleum products combined. Thus, the energy consumption ratio for a given refinery product can be calculated using eq 6:

$$\text{Product Energy Consumption Ratio} = \frac{\left( \frac{1}{\text{Product-Specific Energy Efficiency}} - 1 \right)}{\left( \frac{1}{\text{Refinery Overall Energy Efficiency}} - 1 \right)} \quad (6)$$

The energy consumption ratios from this study can be used in the future to derive product-specific efficiencies from the overall refinery efficiency, which can be calculated from U.S. refining data reported annually by EIA. Such derivation can be justified provided that no major operational changes occur within the U.S. refining industry. By manipulating eq 6 for the energy consumption ratio, we can calculate the product-specific energy efficiency based on the overall refinery efficiency by using the energy consumption ratio of each product, as shown in eq 7:

$$\begin{aligned} \text{Product-Specific Energy Efficiency} \\ = & \left( \left( \frac{1}{\text{Refinery Overall Energy Efficiency}} - 1 \right) \times \text{Product Energy Consumption Ratio} + 1 \right)^{-1} \end{aligned} \quad (7)$$

Figure 10 shows the refinery input (purchased) fuel/blending stock shares that contribute to the total energy consumption for each of the refinery products. The contributions of purchased hydrogen and NG are much higher for diesel, jet fuel, and LPG production compared with gasoline. Furthermore, a significant share of butane and other blending stock (e.g., reformate/alkylate/isomate) contributes to the gasoline pool. Figure 10 also shows that purchased heavy products are primarily processed into clean products (i.e., gasoline, jet fuel, and diesel), while the byproducts of such processing are LPG (processed from FG byproduct), RFO, and coke. Although coke is a less valuable byproduct of the coker unit, it carries a significant energy burden when the coker energy use is distributed among the main (desired) product (diesel) and the less-desired coproducts (RFO and coke) based on their energy values. This anomaly is inherent in the energy allocation method, especially when a less-desirable coproduct is generated in large quantities and at a late stage of the refining process.

**4.2.2.2. Product-Specific Carbon Intensity.** To calculate a product-specific CO<sub>2</sub> emission intensity, we used the amount and carbon content of each process fuel (e.g., NG, FG, FCC coke) to derive the CO<sub>2</sub> emissions from each process unit. We then allocated the CO<sub>2</sub> emissions from each process unit to its product streams based on the energy or market value shares of the product stream (see eq 4). Finally, we aggregated the CO<sub>2</sub> emissions for each stream that reaches a specific product pool using a production-weighted average of the carbon intensity of all

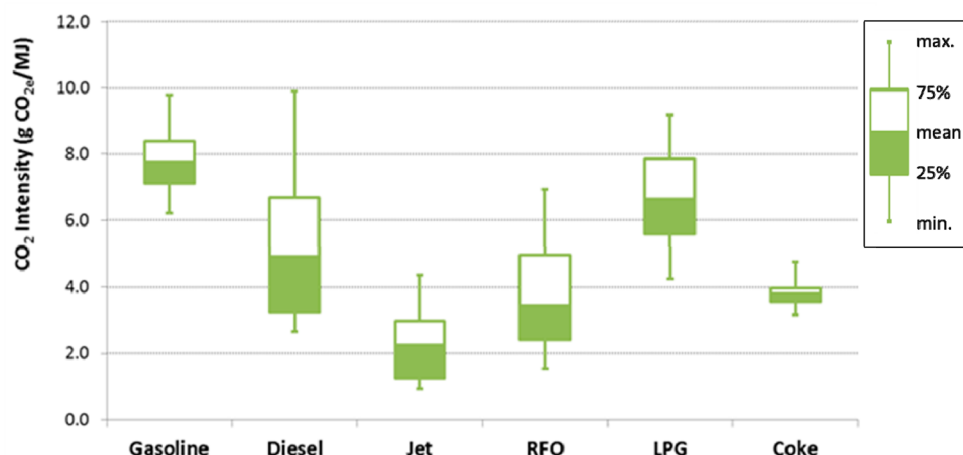


Figure 11. CO<sub>2e</sub> intensity for various products averaged over 43 refineries (with energy allocation method).

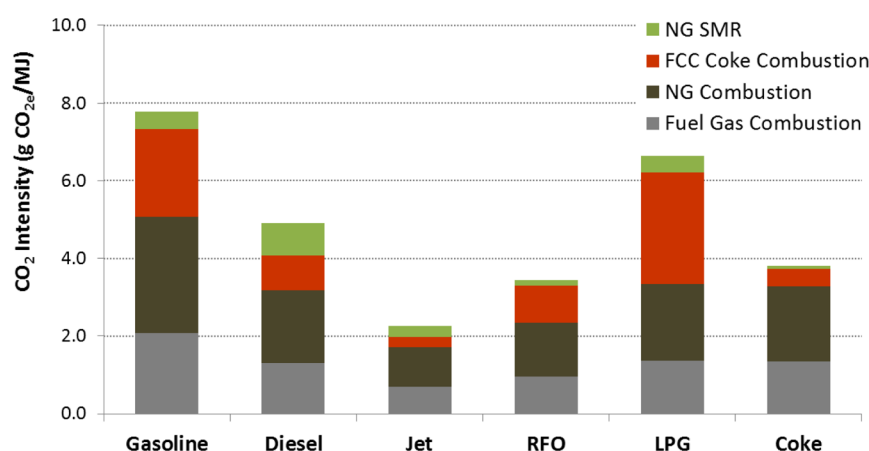


Figure 12. Carbon emission sources for various refinery products averaged over 43 refineries.

streams in that pool. Figure 11 shows GHG emissions intensity in U.S. refineries for various finished products (averaged over the 43 refineries) derived using the energy allocation method. The CO<sub>2e</sub> emissions (in g per MJ) associated with these products and their distributions (i.e., minimum, P25, mean, P75, and maximum values) are consistent with their relative efficiencies (shown in Figure 8). The production-weighted average CO<sub>2e</sub> emissions (in g per MJ) are 7.8 for gasoline, 4.9 for diesel, 2.3 for jet fuel, 3.4 for RFO, 6.6 for LPG, and 3.9 for coke.

The carbon intensity for LPG is higher than that for diesel despite their similar efficiencies. This is attributed to the larger contribution of emissions in the FCC (from catalytic coke combustion) for LPG production compared with diesel production (see Figure 12). This finding is also consistent with the results illustrated in Figure 7, which shows that FCC, which is an energy-intensive process with high carbon emissions, is the main source of LPG; thus, a significant portion of FCC emissions is allocated to LPG. Figure 12 shows that gasoline's burden of carbon emissions from NG SMR hydrogen is lower compared with diesel. This is consistent with the observations of Bredeson et al.<sup>16</sup> Figure 12 indicates that the contribution of NG SMR (for onsite hydrogen production) to the GHG emissions of all products is small, mainly because 27% of the hydrogen used in the 43 modeled refineries is purchased. The GHG emissions associated with the production of purchased hydrogen occur upstream of the refinery (indirect emissions) and are usually

accounted for when conducting life-cycle analysis of the refinery products. Table 3 provides the details of process fuel use per unit fuel produced for major refinery fuel products.

Table 3. Refinery Process Fuel Use for Major Fuel Products (kJ<sub>process fuel</sub>/MJ<sub>fuel product</sub>)

process fuel	gasoline	diesel	jet fuel	RFO	LPG	coke
Purchased Fuels						
NG – SMR	8.81	17.2	5.50	2.64	8.49	1.47
NG – combustion	54.1	35.1	18.8	25.3	36.1	34.9
electricity	4.01	3.24	1.61	1.53	2.98	2.35
H <sub>2</sub>	6.33	13.0	4.33	2.06	7.10	0.879
Internally Produced Fuels						
fuel gas combustion	38.5	22.9	12.5	17.5	25.1	25.1
catalytic coke combustion in FCC	22.5	8.74	2.68	9.57	28.2	4.45

**4.2.3. Life-Cycle Analysis of Refinery Products.** The life-cycle GHG emissions of various refinery products, shown in Figure 13, are dominated by the CO<sub>2</sub> release during fuel combustion at end use. However, the direct refinery-related GHG emissions (i.e., from processing units) and indirect GHG emissions (i.e., upstream emissions associated with the production of purchased

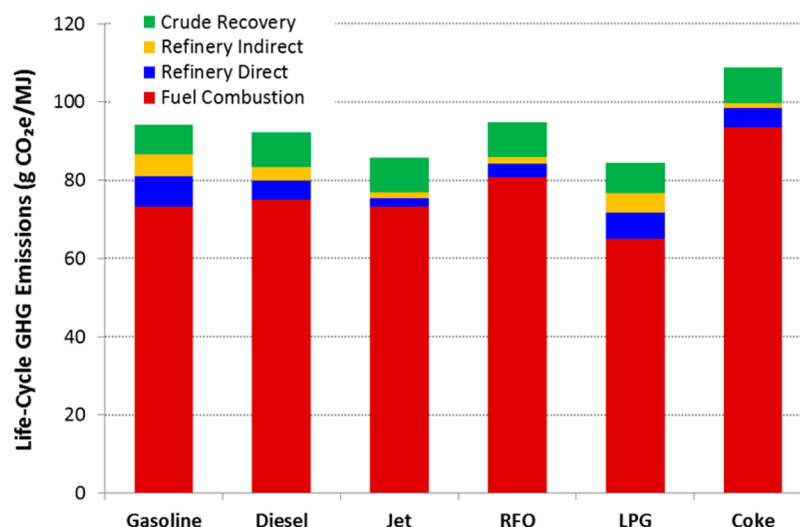


Figure 13. Life-cycle GHG emissions of various refinery products.

hydrogen, steam, and electricity) are also significant, contributing as low as 4% of total life-cycle emissions for jet fuel and as high as 14% of life-cycle emissions for gasoline. The upstream emissions are based on the mix of conventional crude and synthetic crude from oil sands that are fed to U.S. refineries, conventional and shale gas mix for natural gas, and U.S. average electricity generation mix.<sup>20</sup> The total life-cycle GHG emissions for gasoline, diesel, jet fuel, RFO, LPG, and coke are 94, 92, 86, 95, 85, and 109 g CO<sub>2e</sub>/MJ, respectively. The high coke and RFO life-cycle GHG emissions, most of which are released in the combustion phase, are attributed to the high carbon content per unit energy of these fuels. The opposite is true for LPG life-cycle GHG emissions.

## 5. IMPLICATIONS FOR OTHER ANALYSES

The analysis described in this paper served as the basis for another study to evaluate the (1) regional and seasonal variations of energy use and GHG emissions, (2) the impacts of future projections of crude sources/qualities and product slate, and (3) the impacts of growth in the blending of biofuels and synthetic fuels such as FT and renewable diesel/jet with gasoline and distillate fuels, respectively. The findings of that study are documented in another paper (10.1021/es501035a), which has been submitted along with this paper for publication in the same journal.

## ■ ASSOCIATED CONTENT

### 📄 Supporting Information

Additional text, figures, and tables as mentioned in the text. This material is available free of charge via the Internet at <http://pubs.acs.org>.

## ■ AUTHOR INFORMATION

### Corresponding Author

\*E-mail: [aelgowainy@anl.gov](mailto:aelgowainy@anl.gov); phone: 630-252-3074.

### Notes

The authors declare no competing financial interest.

## ■ ACKNOWLEDGMENTS

This research effort by Argonne National Laboratory was supported by the Bioenergy Technologies Office and the Vehicle Technologies Office of the U.S. Department of Energy's Office of

Energy Efficiency and Renewable Energy under Contract DE-AC02-06CH11357.

## ■ REFERENCES

- (1) Energy Information Administration (EIA). *Petroleum Supply Annual 2013 Volume 1, Table 18: Refinery Net Input of Crude Oil and Petroleum Products by PAD and Refining Districts*, 2012; Sept. 27, 2013. <http://www.eia.gov/petroleum/supply/annual/volume1/pdf/table18.pdf>.
- (2) EIA. *Petroleum Supply Annual 2013 Volume 1, Table 17: Refinery and Blender Net Production of Finished Petroleum Products by PAD and Refining Districts*, 2012; Sept. 27, 2013. <http://www.eia.gov/petroleum/supply/annual/volume1/pdf/table17.pdf>, accessed Feb. 14, 2014.
- (3) EIA. *Refinery Capacity Report 2013, Table 10a*; Washington, DC, June 2013.
- (4) U.S. Environmental Protection Agency (EPA). *Greenhouse Gas Reporting Program (GHGRP), Refineries*; Washington, DC, 2012. <http://www.epa.gov/ghgreporting/ghgdata/reported/refineries.html>, accessed Feb. 2014.
- (5) EIA. *Annual Energy Outlook (AEO) 2013, Liquid Fuels Supply and Disposition, Reference Case*; Washington, DC, 2013. <http://www.eia.gov/oiaf/aeo/tablebrowser/#release=AEO2013&subject=0-AEO2013&table=11-AEO2013&region=0-0&cases=ref2013-102312a>, accessed Feb. 2014.
- (6) EPA and National Highway Traffic and Safety Administration (NHTSA). *2017–2025 CAFE GHG Supplemental Rules*; July 29, 2011. <http://www.epa.gov/otaq/climate/documents/420f12051.pdf>, accessed Feb. 2014.
- (7) EPA. *Renewable Fuel Standard (RFS)*; Washington, DC, 2010. <http://www.epa.gov/otaq/fuels/renewablefuels/index.htm>, accessed Feb. 2014.
- (8) Shore, J.; Hackworth, J. Drivers behind growing U.S. product exports and shrinking light-heavy price differences. *Independent Statistics and Analysis* Jan. 2013. [http://www.eia.gov/pub/oil\\_gas/petroleum/presentations/2011/aacsummit/aacsummit.pdf](http://www.eia.gov/pub/oil_gas/petroleum/presentations/2011/aacsummit/aacsummit.pdf), accessed Feb. 2014.
- (9) EPA. *Emission Standards Reference Guide: Highway, Nonroad, Locomotive, and Marine Diesel Fuel Sulfur Standards*. <http://www.epa.gov/otaq/standards/fuels/diesel-sulfur.htm>, accessed Feb. 2014.
- (10) DeGon, S. U.S. Refining Outlook Rosier than It Seems. *Oil Gas J.* 2012, 10, <http://www.ogj.com/articles/print/vol-110/issue-12/processing/us-refining-outlook-rosier-than.html>.
- (11) California Environmental Protection Agency, Air Resources Board. *Low-Carbon Fuel Standard Program*; Sacramento, CA, 2009. <http://www.arb.ca.gov/fuels/lcfs/lcfs.htm>, accessed Feb. 2014.
- (12) Official Journal of the European Union. *Directive 2009/28/EC of the European Parliament and of the Council, on the Promotion of the Use of*



Energy from Renewable Sources; 2009. <http://eur-lex.europa.eu/LexUriServ/LexUriServ.do?uri=Oj:L:2009:140:0016:0062:en:PDF>, accessed Feb. 2014.

(13) Furoholt, E. Life cycle assessment of gasoline and diesel. *Resour., Conserv. Recycl.* **1995**, *14*, 251–263.

(14) Wang, M.; Lee, H.; Molburg, J. Allocation of energy use in petroleum refineries to petroleum products — Implications for life-cycle energy use and emission inventory of petroleum transportation fuels. *Int. J. Life Cycle Assess.* **2004**, *9* (1), 34–44.

(15) Skone, T.; Gerdes, K. *Development of Baseline Data and Analysis of Life Cycle Greenhouse Gas Emissions of Petroleum-Based Fuels*; DOE/NETL-2009/1346; National Energy Technology Laboratory (NETL): Morgantown, WV, Nov. 26, 2008.

(16) Bredeson, L.; Quiceno-Gonzalez, R.; Riera-Palou, X.; Harrison, A. Factors driving refinery CO<sub>2</sub> intensity, with allocation into products. *Int. J. Life Cycle Assess.* **2010**, *15* (8), 817–826.

(17) Keesom, W. H.; Unnasch, S.; Moretta, J. *Life Cycle Assessment Comparison of North American and Imported Crude Oils*; prepared by Jacobs Consultancy and Life Cycle Associates for Alberta Energy Research Institute (AERI), 2009.

(18) Abella, J. P.; Bergerson, J. A. Model to investigate energy and greenhouse gas emissions implications of refining petroleum: Impacts of crude quality and refinery configuration. *Environ. Sci. Technol.* **2012**, *46* (24), 13037–13047.

(19) Hirshfeld, D. S.; Kolb, J. A. Analysis of energy use and CO<sub>2</sub> emissions in the U.S. refining sector, with projections for 2025. *Environ. Sci. Technol.* **2012**, *46*, 3697–3704.

(20) Argonne National Laboratory. *REET1Model 2013*. <http://reet.es.anl.gov/>, accessed Feb. 2014.

(21) Nelson, W. L. Nelson complexity index. *Oil Gas J.* **1976**, *13*, 20–27.

(22) StataCorp LP. *Stata*. <http://www.stata.com/>, accessed Feb. 2014.